J. Cell. Mol. Med. Vol 12, No 5B, 2008 pp. 2037-2051

Mechanical load induced by glass microspheres releases angiogenic factors from neonatal rat ventricular myocytes cultures and causes arrhythmias

D. Y. Barac [a], Y. Reisner [a], M. Silberman [a], N. Zeevi-Levin [a], A. Danon [a], O. Salomon [b], M. Shoham [b], M. Shilkrut [a], S. Kostin [c], J. Schaper [c], O. Binah [a, *]

[a] Rappaport Family Institute for Research in the Medical Sciences, Ruth and Bruce Rappaport Faculty of Medicine, Haifa, Israel
[b] The Faculty of Mechanical Engineering, Technion-Israel Institute of Technology, Haifa, Israel
[c] Max Planck Institute for Heart and Lung Research. Bad Nauheim, Germany

Received: July 26, 2007; Accepted: December 6, 2007

Abstract

In the present study, we tested the hypothesis that similar to other mechanical loads, notably cyclic stretch (simulating pre-load), glass microspheres simulating afterload will stimulate the secretion of angiogenic factors. Hence, we employed glass microspheres (average diameter 15.7 μm, average mass 5.2 ng) as a new method for imposing mechanical load on neonatal rat ventricular myocytes (NRVM) in culture. The collagen-coated microspheres were spread over the cultures at an estimated density of 3000 microspheres/mm^2, they adhered strongly to the myocytes, and acted as small weights carried by the cells during their contraction. NRVM were exposed to either glass microspheres or to cyclic stretch, and several key angiogenic factors were measured by RT-PCR. The major findings were: (1) In contrast to other mechanical loads, such as cyclic stretch, microspheres (at 24 hrs) did not cause hypertrophy. (2) Further, in contrast to cyclic stretch, glass microspheres did not affect Cx43 expression, or the conduction velocity measured by means of the Micro-Electrode-Array system. (3) At 24 hrs, glass microspheres caused arrhythmias, probably resulting from early afterdepolarizations. (4) Glass microspheres caused the release of angiogenic factors as indicated by an increase in mRNA levels of vascular endothelial growth factor (80%), angiopoietin-2 (60%), transforming growth factor-β (40%) and basic fibroblast growth factor (15%); these effects were comparable to those of cyclic stretch. (5) As compared with control cultures, conditioned media from cultures exposed to microspheres increased endothelial cell migration by 15% ($P<0.05$) and endothelial cell tube formation by 120% ($P<0.05$), both common assays for angiogenesis. In conclusion, based on these findings we propose that loading cardiomyocytes with glass microspheres may serve as a new *in vitro* model for investigating the role of mechanical forces in angiogenesis and arrhythmias.

Keywords: mechanical load • ventricular myocytes • hypertrophy • glass microspheres • cyclic stretch • intracellular calcium transients • action potential propagation • arrhythmias

Introduction

Endothelial cells composing the inner most layer of blood vessels experience shear forces exerted by blood flow, which vary in magnitude and pattern, and depend on the flow velocity and vessel geometry. Shear stress changes result in endothelial-dependent vascular restructuring including the formation of new vessels through a process termed arteriogenesis [1]. Additionally, it has been proposed that endothelial cells communicate with their environment, and respond to signals secreted by adjacent tissues including cardiomyocytes [2–7]. In addition to the mechanical load-responsive endothelial cells, studies have shown that cardiomyocytes also participate in the angiogenic response to mechanical forces. For example, Tomanek's group [6] has shown that in neonatal rat ventricular myocytes (NRVM) exposed to cyclic stretch, the expression of vascular endothelial growth factor (VEGF) and transforming growth factor-β (TGF-β) was increased. In recent years several experimental models have been utilized to impose mechanical load on cardiomyocytes, the most frequently used were those employing static stretch [8–11] and pulsatile

*Correspondence to: Ofer BINAH,
Rappaport Institute, Efron Street
P.O.B 9697, Haifa 31096, Israel
Tel.: +972-4-8295262
Fax: +972-4-8513919
E-mail: binah@tx.technion.ac.il

doi:10.1111/j.1582-4934.2007.00193.x

cyclic stretch [12–14]. In general, stretching (static or cyclic) cardiomyocytes increases protein synthesis without altering DNA synthesis (*i.e.* inducing hypertrophy) or gene expression [8, 14]. In both models, myocytes are plated on an elastic membrane and stretched to a longer resting length, statically or in a cyclical manner. Hence, in these models the stretch is not synchronized with the contraction of the myocytes, and therefore the load imposed on the myocytes is of a mixed nature, combining both preload and afterload.

In an attempt to distinguish between the angiogenic effects of preload and afterload, and to determine the effect of the latter on the secretion of angiogenic factors by cardiomyocytes, we utilized a novel method to mechanically load myocytes during contraction, thus simulating the *in vivo* settings of afterload. As will be described herein, the afterload was induced by spreading on NRVM glass microspheres that adhered to the myocytes and acted as small weights carried by the cells during their contraction [15]. Using this model we found that whereas microspheres did not cause hypertrophy or changed Cx43 expression and conduction velocity, the microspheres increased the expression of several key angiogenic factors, which are likely to contribute to the mechanical load-induced angiogenesis.

Methods

Cell cultures

The research conforms to the Guide for the Care and Use of Laboratory Animals published by the US National Institutes of Health (NIH publication no. 85-23; revised 1996).

(i) NRVM cultures prepared as previously described [16] were studied 4–6 days after plating. Twenty four hours before the actual experiment, the cultures were transferred to serum-free medium with 50%/50% DMEM/F-12 (Biological Industries, Beit Haemek, Israel) containing 2 mM L-glutamine, 0.1 mmol/l BrdU, ITS (Insulin-transferine-sodium selenite media supplement (Sigma) and penicillin.

(ii) *Primary Bovine Aortic Endothelial Cells (BAEC).* BAEC were prepared as previously described [17] from bovine aortas.

Mechanical load induced by glass microspheres or cyclic stretch

Mechanical load was induced in different NRVM cultures either by cyclic stretch or glass microspheres.

(i) The cyclic stretch apparatus. NRVM were exposed to cyclic stretch by an apparatus (Fig. 1A) generously donated to us by Dr. André Kléber (Department of Physiology, University of Bern, Bern, Switzerland). A comprehensive description of the apparatus is provided in ref. 14. In brief, NRVM were plated onto the surface of a rectangular sheet of silicone membrane (thickness 0.01 inch), the borders of which are fixed to Teflon bars that can move freely in the *x* direction along two stainless steel axes. The two bars are in contact with an elliptical Teflon wheel mounted in the centre of the apparatus. The silicone membrane was cut to a length that produced tension slightly above the slack length when the short diameter of the wheel is in contact with the Teflon bars. The 1.1/1 ratio of the long to the short diameter of the elliptical wheel produced stretch of 10% during a 90° rotation of the wheel. In the present work, the frequency of the stretch pulsations (half a wheel cycle) was 3 Hz.

(ii) Glass microspheres. Glass microspheres (Duke Scientific Corporation, Palo Alto, CA, USA) were coated with collagen type 1 and spread over spontaneously contracting cultured NRVM. The reason for coating the microspheres with collagen type 1 was that this molecule is the predominant matrix protein of the normal heart. Furthermore, Shaker and co-workers have shown that cyclic stretch (applied by the same device used here) induced a ~2-fold increase in Cx43 expression in NRVM grown on native collagen but no increase in cells grown on fibronectin or denatured collagen. Since the effect of mechanical load on Cx43 expression was one of the end points of this study, we limited ourselves to this type of coating [18]. The physical properties of the glass microspheres are: specific gravity; 2.4 g/cm^3, mean diameter; 15.7±1.1 μm, average mass of each sphere; 4.02 ng. Shortly after applying the microspheres to the cultures, they strongly adhered to the myocytes surface (Figs. 1B and C), and moved simultaneously with the contracting myocytes, thus applying afterload as discussed above. Twenty four hours before application, the microspheres were sterilized for 2 hrs in ethanol 70%, washed in PBS and immersed overnight in collagen (4 mg/ml) type I solution (Sigma C-8919) diluted 1:10 in 1 mM acetic acid. Immediately before application, the microspheres were washed with phosphate buffer saline (PBS) and re-suspended in the culture medium. Microspheres were applied at a density of ~3000 microspheres/mm^2, so that when evenly distributed, there were 1–2 microspheres per a small number of cells (Figs. 1B and C).

Measurement of intracellular calcium transients and myocytes contraction

Intracellular Ca^{2+} ($[Ca^{2+}]_i$) transients were measured by means of Fura-2 fluorescence and the DeltaScan system (Photon Technology International, PTI) as previously described [19]. In these experiments, cardiomyocytes were stimulated using platinum wires embedded in the walls of the perfusion chamber.

Extracellular electrograms recordings using the Micro-Electrode-Array data acquisition system

Unipolar electrograms were recorded from NRVM plated on Micro-Electrode-Arrays (MEA; see Fig. 5A) using the MEA60 system (Multi Channel Systems, Reutlingen, Germany), as previously described [20, 21]. For the electrophysiological measurements, MEAs were removed from the incubator, placed in the recording apparatus preheated to 37°C, and electrograms were recorded within 1–3 min. To ascertain that these measurements were performed within the stable period, in addition to the 1–3 min. time points, conduction velocity was measured at 8 and 10 min after removing the cultures from the incubator. As we previously reported [21], in control cultures, conduction velocities, normalized to the value measured at ~2 min., were respectively: 1.02±0.01 at 8 min and 1.03±0.01 at 10 min. Cultures were paced (STG-series, Multi Channel Systems) *via* one of the four pairs of bipolar stimulating electrodes (250 μm × 50 μm) (Fig. 5C), left panel), by delivering rectangular biphasic impulses (duration 2–3 ms; ×2 threshold intensity) at different stimulation rates. The electrogram analysis was performed automatically using custom-made MATLAB

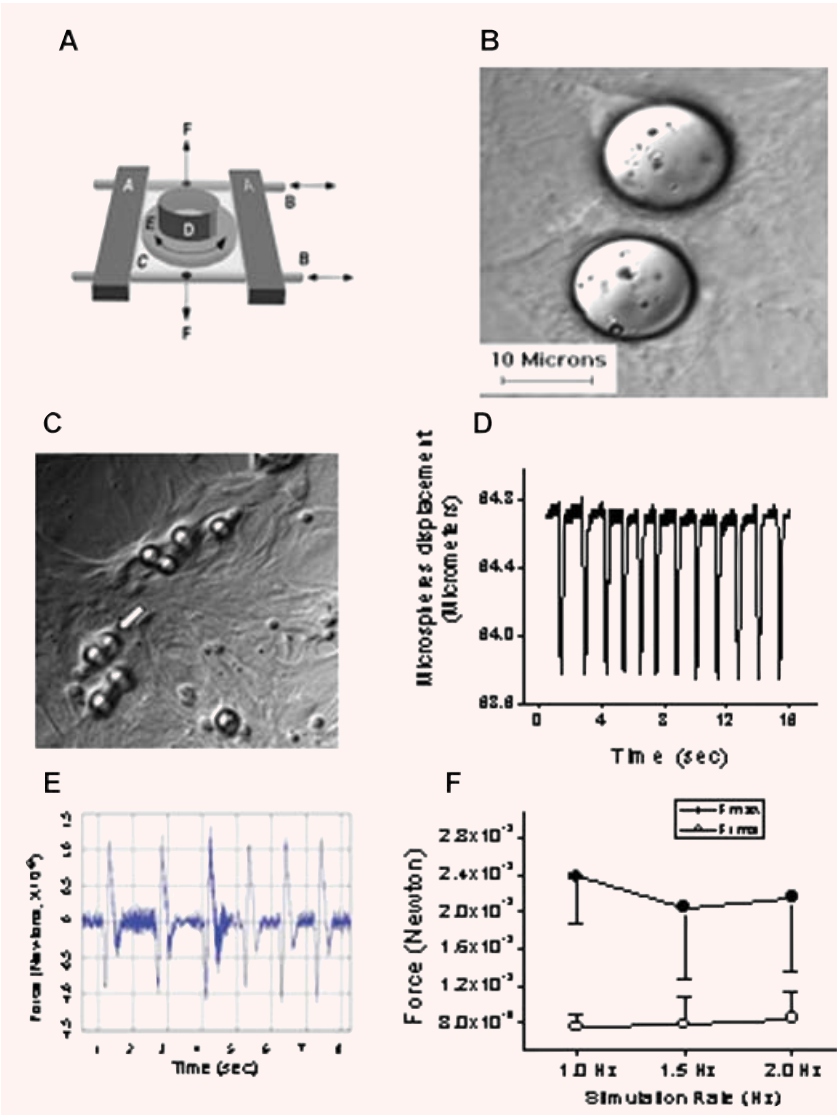

Fig. 1 The experimental procedures for inducing mechanical load by means of cyclic stretch and glass microspheres in neonatal rat ventricular myocytes (NRVM) cultures. [**A**] Adopted from Ref. 14. Schematic presentation of the cyclic stretch apparatus designed and built by Dr. André Kléber (Department of Physiology, University of Bern, Bern, Switzerland). Horizontal metal bars (**A**) glide horizontally on stainless cylindrical axes (**B**) and support the transparent silicone membrane (**C**). A segment of silicone tubing (**D**) was glued on the silicone membrane to form the walls of the culture dish in which the neonatal rat myocytes were seeded and grown. Two clamps (**F**; positions indicated by vertical arrows) produced slight tension along the central axis of the stretch apparatus and thereby reduced transverse shrinking to $<1\%$. [**B**] Microspheres are spread on the culture. [**C**] Cells adhere to the collagen coated microspheres, sometimes completely covering them (white arrow), to form a single contracting unit. [**D**] Representative displacement recording of a single microsphere, obtained by means of a video edge detector. [**E**] Calculated force/time relationship from the displacement graph shown in panel D. [**F**] The force generated at different stimulation rates (n = 4–6 myocytes). Fmax, maximal force; Frms, root mean squares of force over time.

(MATLAB® 6.5) routines. The local activation time (LAT) at each electrode, defined as the time of occurrence of the first derivative plot minimum of the fast activation phase (Fig. 5B), was used to construct activation maps and calculate conduction velocity. The scalar value of the local conduction velocity was calculated at each of the array electrodes as previously described [20, 21]. The value of conduction velocity presented for each measurement was taken as the mean value of local velocities of all 60 electrodes.

Cell migration assay

The migration assay was performed by means of the 'cellular injury test' [22]. Briefly, BAEC were plated to confluence on a gelatin-coated 96-well plate in a growth medium. Twenty four hours after plating, a wound was performed by scraping the cells in half of each well with a sterile wooden stick. The cells were rinsed with growth medium, and 200 µl of conditioned medium obtained from control cultures, or from cultures exposed to microspheres or cyclic stretch for 24 hrs, was added to each well. To prepare conditioned medium, the medium from each experiment was collected, centrifuged for 5 min. and the supernatant was kept at $-20^{\circ}C$ and thawed just before use in the migration assays. The distance from the cells in front to the edge of each well was determined using a phase-inverted microscope equipped with a calibrated eyepiece. The migration rates 24 hrs after inducing the wound were calculated for each well. The effect of the conditioned medium from the treated cultures was expressed as fold of the control conditioned medium.

Angiogenesis assessed by tube formation assay

Tube formation of BAEC was conducted as an assay of *in vitro* angiogenesis, as previously described [23]. Briefly, a 24-well plate was coated with 350 µl of Matrigel (Becton Dickinson Labware, Bedford, MA, USA) and was

Table 1 PCR primers and protocols

Genes	Primers	PCR protocol
ANP	Up: 5′- ATG GGC TCC TTC TCC ATC ACC -3′	94°C 30 sec., 58°C 30 sec., 72°C 1 min.
	Down: 5′- GTA CCG GAA GCT GTT GCA GCC -3′	35 cycles
VEGF	Up: 5′- CCAGCACATAGGAGAGATGAGCTTC -3′	94°C 20 sec., 55°C 30 sec., 72°C 1 min.
	Down: 5′- GGTGTGGTGGTGACATGGTTAATC -3′	30 cycles
b-FGF	Up: 5′- ACACGTCAAACTACAACTCCA -3′	94°C 15 sec., 55°C 15 sec., 72°C 30 sec.
	Down: 5′- TCAGCTCTTAGCA GACATTGG -3′	35 cycles
TGF-β	Up: 5′- CTAAGGTGGACCGCAACAAC -3′	94°C 15 sec., 55°C 15 sec., 72°C 30 sec.
	Down: 5′- CGGTTCATGTCATGGATGGG TG -3′	35 cycles
Ang-2	Up: 5′- GCAACGAGTT TGTCTC -3′	94°C 45 sec., 55°C 45 sec., 72°C 1 min.
	Down: 5′- ACTTTATTCGTATTCTGCTTT -3′	35 cycles
β-actin	Up: 5′-GCCATGTACGTAGCCATCCA -3′	94°C 20 sec., 55°C 30 sec., 72°C 1 min.
	Down: 5′-GAACCGCTCATTGCCGATAG -3′	30 cycles

allowed to solidify at 37°C for 1 hr. BAEC were seeded on the Matrigel (3×10^4 cells per well) and cultured in the presence of 200 µl of conditioned medium (from control or treated cultures). The effect of the conditioned media (following 5 hrs incubation) on the formation of new networks of tubes was expressed as the number of tubes counted in three fields, in three different wells, and photographed after 5 hrs.

Morphological, molecular and immunofluorescence analyses

(i) Immunohistochemical staining and analysis. For immunostaining, cultures plated on glass cover slips were rinsed with PBS, fixed for 10 min. in 4% paraformaldehyde in PBS at room temperature and permeabilized on ice with 0.2% Triton X-100 (Sigma) in PBS. The cultures were blocked with normal goat serum 10% (Biological Industries, Beit Haemek, Israel) for 1 hr at 37°C. The primary antibodies used in this study were: mouse monoclonal anti-α-actinin (Sarcomeric) (clone EA-53, Sigma), and mouse monoclonal anti-Cx43 antibody (MAB 3068; Chemicon International, Temecula, CA, USA). Secondary antibodies used were CY2-conjugated goat antimouse IgG conjugated with CY5 (Jackson ImmunoResearch Laboratories, West Grove, PA, USA) for α-actinin and CY5-conjugated donkey antimouse IgG (Chemicon International) for Cx43. After blocking, preparations were incubated overnight at 4°C with the primary antibody. Subsequently, the cultures were rinsed extensively and incubated with the secondary antibody for 1 hr at room temperature. Nuclei were stained using ToPro (Molecular Probes). F-actin was stained with phaloidin-conjugated with Alexa 488 (Molecular Probes).

Confocal microscopy was performed by means of a confocal scanning laser microscope (Radiance 2000 confocal, Bio-Rad) connected to a Nikon e600 upright microscope. Analysis was performed using Image-Pro® Plus version 5 software (MediaCybernetics, Silver Spring, MD). Each recorded image (150 µm × 150 µm) was obtained using multi-channel scanning, and consisted of 1024 × 1024 pixels (150 µm × 150 µm). All cultures were immunolabelled simultaneously using identical dilutions of primary and secondary antibodies, and scanned under identical scanning parameters. The cellular area was defined as the positive α-actinin-labelled area exceeding the threshold of 15 on the 0–255 grey intensity scale. The α-actinin stained area was automatically identified by the Image-Pro software, which measured the occupied stained area within the microscopic field. For Cx43 analysis, the threshold parameters were chosen and set in the Image-Pro so that only the densely fluorescence spots representing Cx43 immunostained gap junctions were selected. The same threshold parameters were used throughout the analysis. After selecting all gap junctions in a field, the fluorescence intensity of each point, the area of individual gap junctions and the total number of gap junctions per field, as well as the total fluorescence intensity (of all selected gap junctions in the field) were determined.

(ii) Protein expression analysis by Western blot. Western blot analysis of Cx43 protein expression was performed on lysates treated with phosphatase and protease inhibitors as described previously [21]. Monoclonal anti-Cx43, recognizing total-Cx43 (Chemicon International, Temecula, CA, USA) or monoclonal anti-Cx43, recognizing nonphosphrylated-Cx43 (NP-Cx43) (Zymed Laboratories, San Francisco, CA, USA) antibodies were used. Immune complexes were detected using the enhanced chemiluminescence detection system (Perkin Elmer Life Sciences, Boston, MA, USA) with a secondary antibody coupled to horseradish peroxidase (Jackson ImmunoResearch Laboratories, West Grove, PA, USA), followed by autoradiography. Cx43 band intensity was quantified by densitometry and normalized to total actin (Chemicon).

(iii) mRNA determination by RT-PCR. Total RNA was extracted from NRVM cultures using the EZ-RNA™ isolation kit (Biological Industries, Beit-Haemek, Israel) according to the manufacture's protocol, and the Reverse Transcriptase (RT) reaction was conducted as described previously [24], using specific primers (Table 1). The PCR reaction was carried out under the following conditions. An initial denaturation step at 94°C for 2 min. for all primers, followed by a final elongation step at 72°C for 10 min. The amplified products were analysed by 2% agarose gel and visualized using ultra violet fluorescence after staining with ethidium bromide. The relative levels of mRNA encoding the above products were quantified by densitometry and normalized to β-actin mRNA.

Statistical Analysis

The results are presented as mean ± S.E.M. Comparison between multiple continuous parametric groups was performed using the two-way ANOVA test, followed by the Bonferroni *post-hoc* test. Comparison between two parametric groups was performed using the Student's t-test for independent groups. Paired t-test was performed for studying cells before and after treatment. *P* values of 0.05 or less were considered statistically significant.

Results

The experimental model of loading NRVM with glass microspheres

Since this is the first report respecting the effects of glass microspheres on NRVM, we describe in depth the changes in morphological, molecular and functional aspects of NRVM, prior to demonstrating that the mechanical load induced by the microspheres releases angiogenic factors. As described in the Methods section, the collagen-coated microspheres strongly adhere to the myocytes (Fig. 1C), and thus move uniformly with the cell surface. Under these circumstances, the force applied by a single microsphere on the myocyte can be calculated by measuring the microsphere displacement during the myocyte contraction. As shown by a representative experiment (Fig. 1D), the microsphere displacement was measured using a video edge detector routinely used for measuring myocyte contraction [19]. The force acting on the microsphere was calculated by multiplying the acceleration by the microsphere mass ($F = m \times a$) (see the Methods section for the microspheres physical properties). The microsphere acceleration is the second time derivative of the displacement = m/s^2. Figure 1E depicts a representative calculated force curve of a microsphere in a culture stimulated at 1 Hz. Figure 1F shows the force calculated as the values of the maximal force (Fmax) for each cycle and the root mean squares (Frms) of the forces during a complete cycle.

Do glass microspheres cause hypertrophy?

Since various experimental models of mechanical load, including cyclic stretch cause myocyte hypertrophy [25, 26], we initially determined whether glass microspheres also cause hypertrophy of NRVM.

Cell area measured by α-actinin fluorescence

The first marker measured was cell area, which is commonly used to assess hypertrophy [27–30]. As described in the Methods section, cell area represented by α-actinin immunofluorescence staining (Fig. 2A) was measured from cultures in which myocytes were plated at a low density. As seen in Figure 2B, while cell surface area increased in both groups during the 24 hrs period ($P<0.05$), no difference was found between the control and the microspheres-treated cultures.

The effect of microspheres on ANP mRNA levels

A common molecular marker of hypertrophy is atrial natriuretic peptide (ANP), which was shown to be increased by hypertrophic stimuli such as biomechanical load [27], Fas receptor activation [24], angiotensin II, endothelin-1 and norepinephrine [31–33]. In agreement with the lack of change in cell area (Fig. 2B), exposure to microspheres for 24 hrs did not increase ANP levels (Fig. 2C), collectively suggesting that the mechanical load induced by microspheres does not cause hypertrophy of NRVM.

The effect of microspheres on Cx43

Based on the studies showing that cyclic stretch (at 1 and 6 hrs) in NRVM caused a dramatic up-regulation of Cx43 signal and protein expression (14, 18), we tested whether a similar effect is caused by glass microspheres. Figure 2D depicts representative Western blots for total Cx43 (top), NP-Cx43 (middle) and actin (bottom) for cultures exposed to microspheres for 24 hrs *versus* corresponding control cultures. The total Cx43 antibody recognizes three bands: two major bands at 44 and 46 kD that comprise two phosphorylated isoforms, and another band at 41 kD that comprises the NP Cx43. Figures. 2E & 2F depict the summary of the densitometry analysis for total-Cx43 and NP-Cx43, respectively. In contrast to the effect of cyclic stretch on Cx43 [14, 18, 34], and in accordance with the absence of hypertrophy (Figs. 2B and C), microspheres did not increase the expression of total or NP-Cx43 (Figs. 2E and F). Next, we analysed gap junctional morphological properties as derived from Cx43 immunofluorescence staining of control and microspheres-treated cultures (Fig. 3A). Thus, the microspheres did not affect the number of gap junctions per microscopic field (150 μm × 150 μm) (Fig. 3B), or the percent of the microscopic field occupied by Cx43 gap junctions (Fig. 3C). Further, quantitative analysis revealed no differences in the mean fluorescence intensity of Cx43 either per microscopic field (Fig. 3D) or per individual gap junctions (Fig. 3E).

The effect of microspheres on the $[Ca^{2+}]_i$ transients and action potential propagation

The effect of microspheres on $[Ca^{+2}]_i$ transients

To further characterize this novel experimental model, we tested the effects of microspheres on the $[Ca^{+2}]_i$ transients (a representative recording is depicted in Fig. 4C), which were shown to be affected by experimental mechanical load [35, 36]. $[Ca^{2+}]_i$

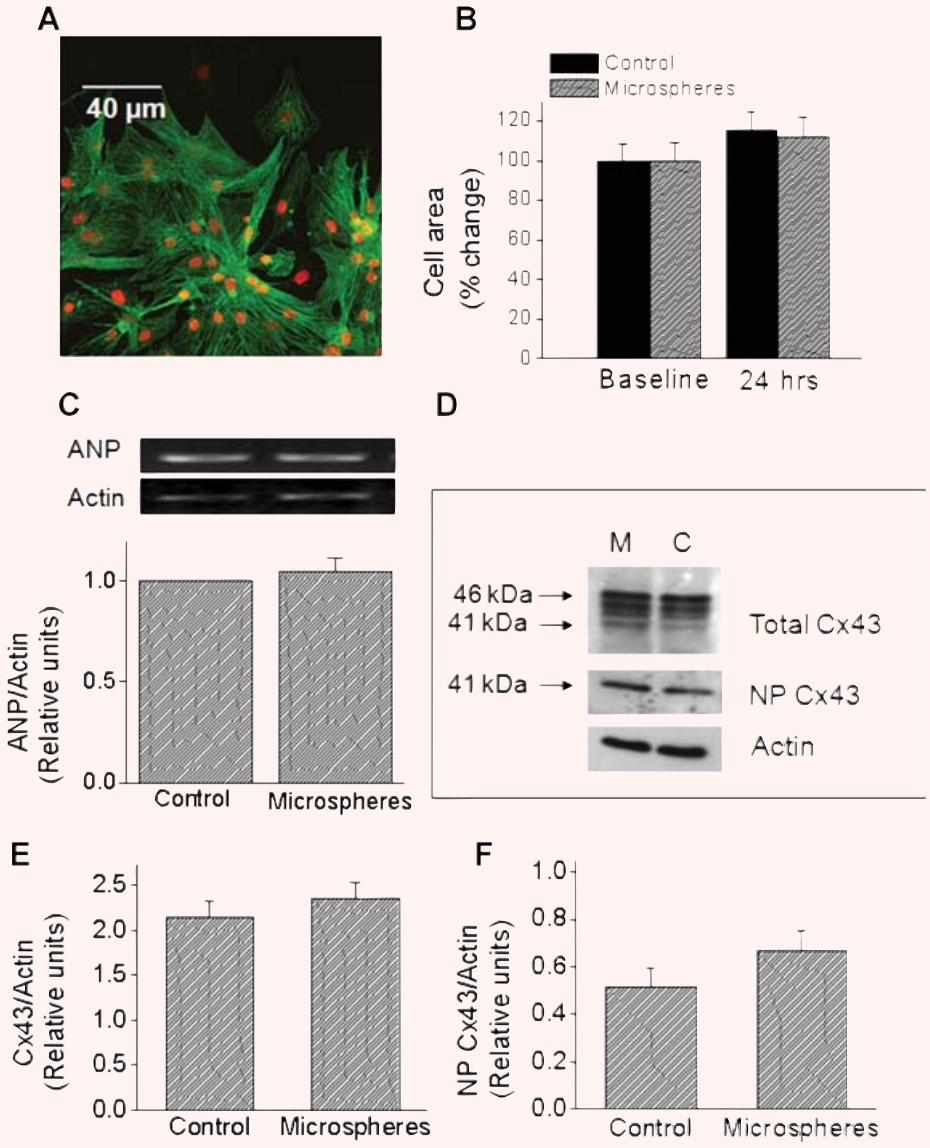

Fig. 2 The effects of glass microspheres on cell area, atrial natriuretic peptide (ANP) mRNA levels and Cx43 protein expression. (**A**) Immunofluorescence analysis of cell area. A representative picture showing combined α-actinin and ToPro. Magnification ×400. (**B**) Summary of the cell area analysis based on α-actinin immunofluorescence staining. In both groups, cell area was similarly increased after 24 hrs. Control, n = 24 cell groups; microspheres, n = 28 cell groups. At 24 hrs the cell area was expressed as percent change from control (baseline). (**C**) Microspheres do not increase ANP mRNA. The upper panel depicts representative blots, and the lower panel depicts quantitative densitometric analysis from control cultures and from cultures treated for 24 hrs with microspheres (n = 5). Each value was divided by its corresponding actin value. Values are normalized to control cultures, which are set as 1.0. (**D**)–(**F**) Effects of microspheres on Cx43 protein expression. (**D**) Representative Western blots for control (**C**) and microspheres (M) treated cultures. Samples were probed for total Cx43 (upper panel) and NP Cx43 (middle panel). Equivalency of loading was verified with an antibody against actin (lower panel). Upper and lower arrows indicate the positions of the 46 and 41 KD bands, respectively. (E and F) Quantitative densitometric analysis of total Cx43 and NP Cx43 expression, respectively. Each value was divided by its corresponding actin value. Control, n = 16 samples; Microspheres, n = 15 samples (each sample is a pull of 2–3 cultures).

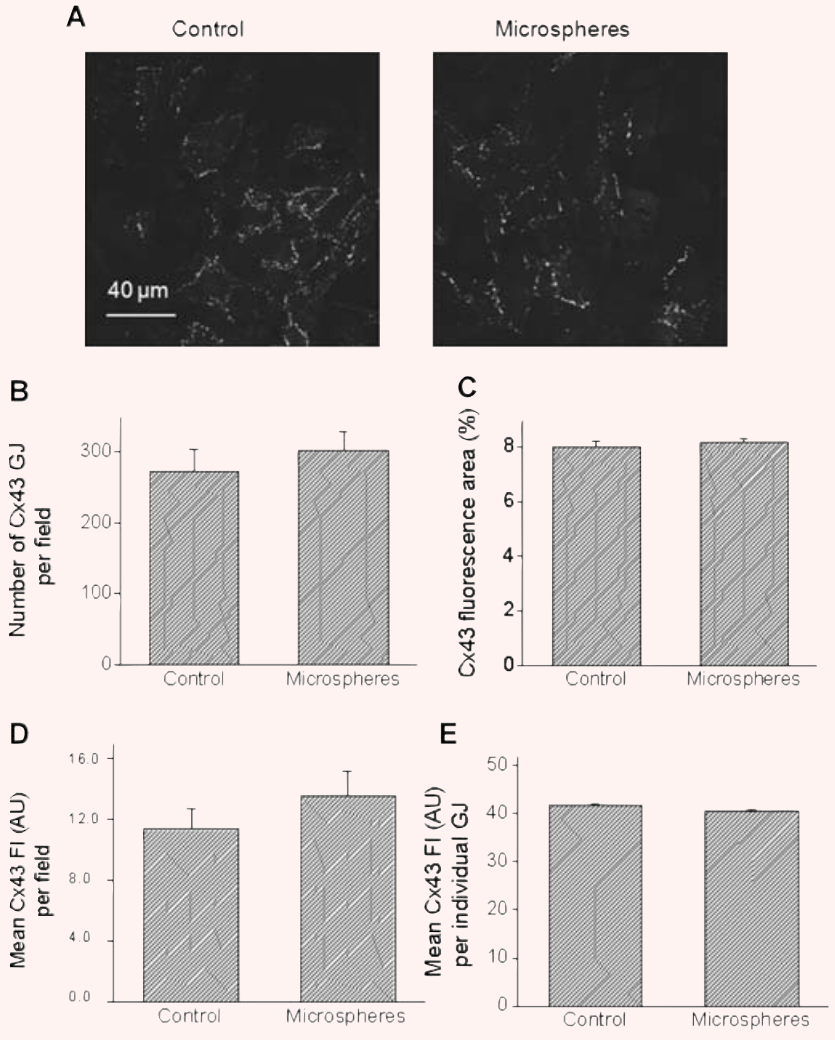

Fig. 3 Quantitative analysis of confocal microscopy images of cultures stained for Cx43. (**A**) Representative confocal images of a control culture (left), and a culture exposed for 24 hrs to microspheres (right). Scale bar = 40 µm. (**B**) Number of Cx43 gap junctions (GJ) per microscopic field. (**C**) Percent of microscopic field occupied by Cx43 positive signal. Mean fluorescence intensity (FI) of Cx43 expressed as arbitrary units (AU) per microscopic field [**D**] or per each GJ [**E**]. Control, n = 8 fields; Microspheres, n = 10 fields.

transients were recorded from cultures stimulated at 0.5, 1.0, 1.5 and 2.0 Hz. As shown in Figure 4A, the diastolic and the systolic $[Ca^{2+}]_i$ fluorescence ratios were higher in the microspheres group than in the control group. In addition, the rate of $[Ca^{2+}]_i$ relaxation was slower in the microspheres-treated group compared to control cultures (Fig. 4B). This decrease in the rate of $[Ca^{2+}]_i$ relaxation (representing removal of free Ca^{2+} ions from the cytosol) may result in elevation of diastolic $[Ca^{2+}]_i$, which may promote arrhythmias [37]. Indeed, as compared to control cultures (a representative culture is depicted in Fig. 4C), the $[Ca^{2+}]_i$ transients recorded from NRVM treated for 24 hrs (but not for 1 hr) with microspheres frequently demonstrated arrhythmias. Since these arrhythmias disappeared as stimulation rate was increased (an example shown in Fig. 4D), it is likely that they resulted from early afterdepolarizations. In summary, while only one out of the 20 (5%) control cultures had arrhythmias, three of the seven microspheres-treated cultures were arrhythmogenic (42%, $P<0.05$ *versus* control, Fisher exact test).

The effect of microspheres on action potential propagation

An important functional aspect of NRVM which was shown to be affected by biomechanical load such as cyclic stretch [14] is conduction velocity. In the present study we measured action potential

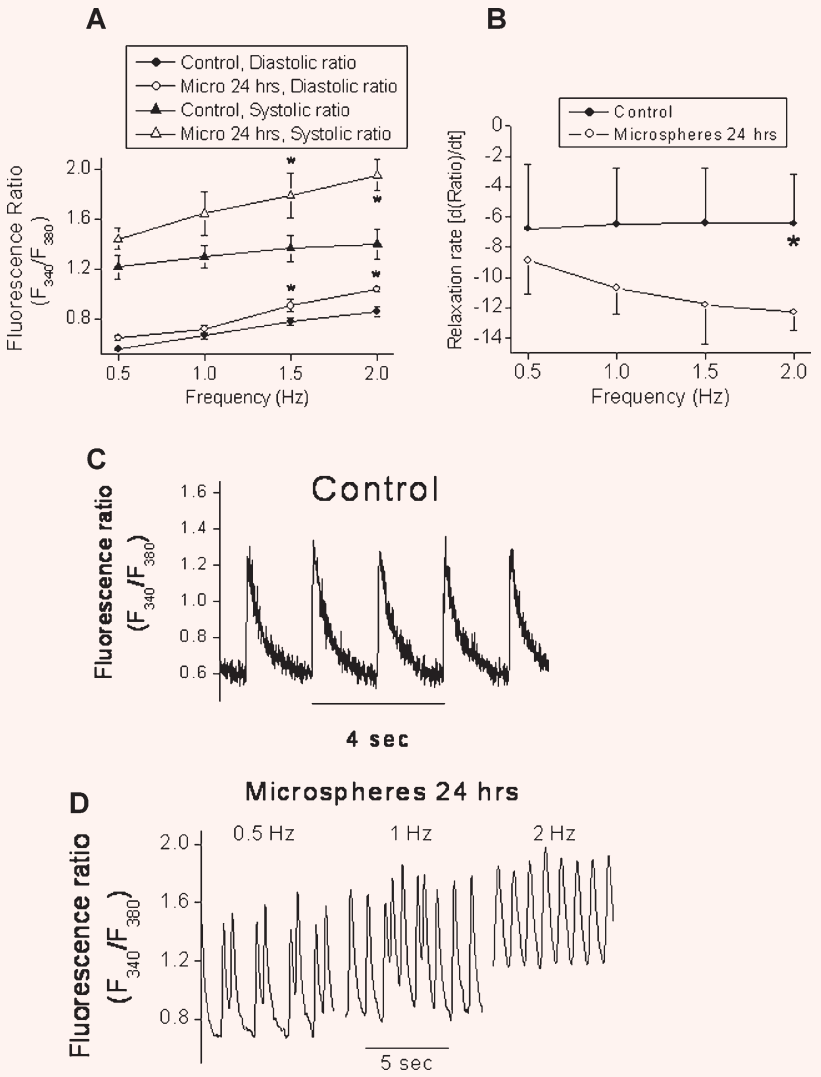

Fig. 4 The effect of glass microspheres (24 hrs) on $[Ca^{+2}]_i$ transients. (**A**) The diastolic and systolic fluorescence ratios recorded from NRVM stimulated at 0.5, 1.0, 1.5 and 2.0 Hz. (**B**) The rate of $[Ca^{+2}]_i$ relaxation in $[Ca^{+2}]_i$ transients generated at 0.5, 1.0, 1.5 and 2.0 Hz. $^*P<0.05$, n = 6 for control, n = 4 for microspheres. (**C**) Representative $[Ca^{+2}]_i$ transients in control and microspheres-treated cultures (**D**). Panel **D** shows the disappearance of the arrhythmias as the stimulation rate is increased.

propagation from electrically-confluent NRVM cultures by means of the MEA data acquisition system, which is based on non-invasive electrogram measurements from NRVM plated on a matrix of electrodes, 30 μm in diameter and 200 μm apart (Fig. 5A). As shown in Figure 5B, the extracellular electrogram is composed of a fast activation phase resulting from action potential upstroke, and from a pseudo T-wave resulting from the repolarization phase of the action potential. As previously described [20, 21] colour-coded activation maps were generated by calculating the mean LAT from three consecutive action potentials (Fig. 5C), where the red denotes early activation and the blue late activation. Hence, in this culture, action potential originated at the stimulating electrodes (represented by the two black rectangles) and propagated upward, crossing the electrode array within ~8 ms (see colour-coded bar below the activation map). As seen by the conduction velocities values beneath the maps (Fig. 5C) and by the summary figure (Fig. 5D), in agreement with the current work showing that microspheres did not cause hypertrophy, exposure of NRVM to microspheres for 3, 6 and 24 hrs did not affect the activation patterns or conduction velocity. This finding also suggests that the microspheres did not adversely affect the functionality of NRVM.

Secretion of angiogenic factors by microspheres and cyclic stretch

To test the hypothesis that mechanical load imposed by microspheres releases angiogenic factors, we determined whether the

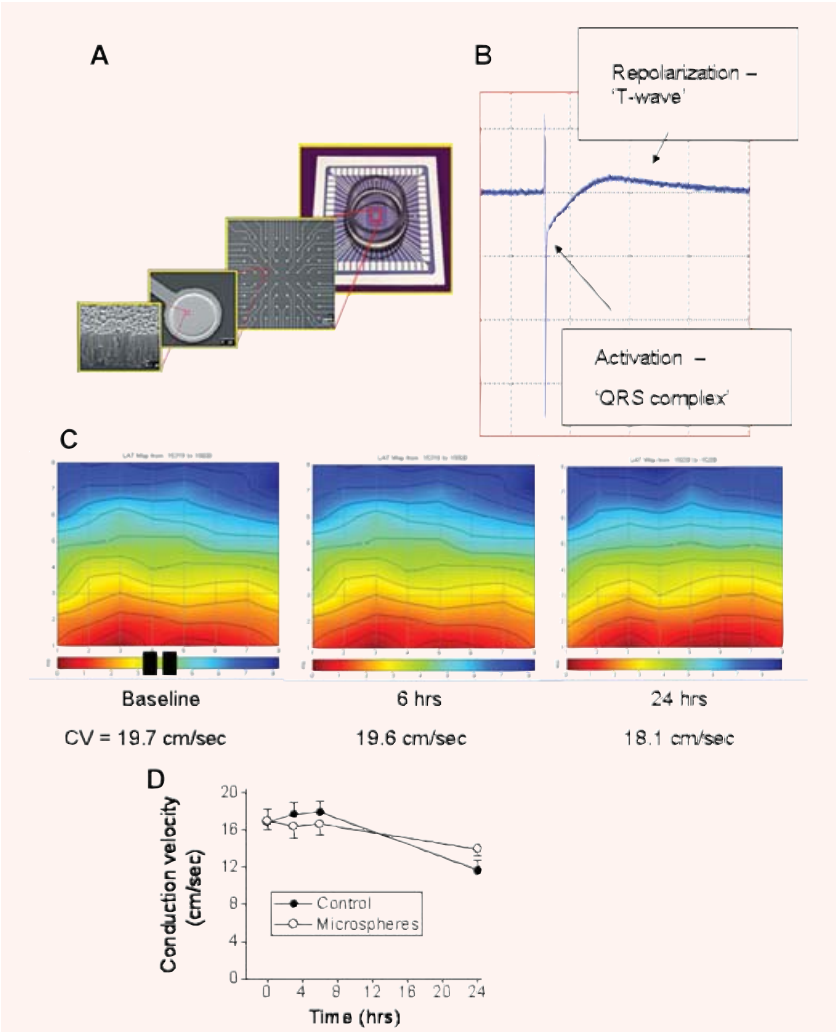

Fig. 5 Electrophysiological recordings from control and microspheres-treated NRVM cultures, using the Micro-Electrode-Array data acquisition system. (**A**) A description of the electrodes layout, and microscopic structure. (**B**) A representative electrogram depicting the two major phases: fast activation ('QRS-complex') and a slow phase corresponding to the repolarization of the action potential. (**C**) Representative colour-coded activation maps from a control culture at baseline, 6 hrs and 24 hrs. The black rectangles at the bottom of the left map denote the stimulating electrodes. The corresponding conduction velocities (see Methods for details) are depicted below the maps. (**D**) A summary of the conduction velocity of control cultures (n = 16) and microspheres-treated cultures (n = 15) during a 24-hrs follow-up period.

expression of VEGF (a key angiogenic factor) is increased. Since we could not detect VEGF protein message (using Santa Cruz antibody SC 507, n = 10 experiments, with different Western blotting conditions), we reverted to measuring VEGF mRNA (using RT-PCR) [7, 38] in NRVM exposed to microspheres for 3, 6, 12 and 24 hrs. In agreement with previous reports [6], as shown in a representative control experiment (Fig. 6A) VEGF transcripts appeared as four bands: 121, 145, 165 and 189 KB. To determine which of the VEGF isoforms are represented by these bands, the product of PCR reactions of 5 plasmids encoding the five VEGF isoforms (121, 145, 165, 189 and 201 KB) were analysed by electrophoresis. According to the migration pattern of the five isoforms (Fig. 6B) we concluded that in NRVM cultures, the upper doublets PCR products represent the 165 KB and 185 KB isoforms and the lower doublets represent the 121 KD and 145 KD isoforms. Since: (1) not in all of the cultures a satisfactory separation of the VEGF isoforms could be obtained, and (2) we could not detect one isoform that was dominant over the others, the level of VEGF expression was analysed as a cumulative result of all 4 bands. As seen in Figure 6C, in support of the hypothesis, microspheres increased the VEGF mRNA levels, peaking at 6–12 hrs and then decreasing at 24 hrs.

Based on the finding that VEGF mRNA expression was increased by exposure to microspheres for 24 hrs, we determined how the expression of additional key angiogenic factors, angiopeitin-2 (Ang-2), tumour growth factor-β (TGF-β) and basic fibroblast growth factor (b-FGF) are affected by microspheres (24 hrs exposure). As seen in Figure 6 microspheres significantly ($P<0.05$) increased the expression of Ang-2 (Fig. 6D) and TGF-β (Fig. 6E), but not of b-FGF (Fig. 6F). For comparison, we determined the effect of cyclic stretch applied at 3 Hz for 24 hrs, and found that it increased ($P<0.05$) the expression of Ang-2, TGF-β and b-FGF (Figs. 6D–F). We also attempted to detect angiopoeitin-1 (a ligand for the Tie2 receptor) expression in NRVM, but its low expression did not allow a reliable analysis.

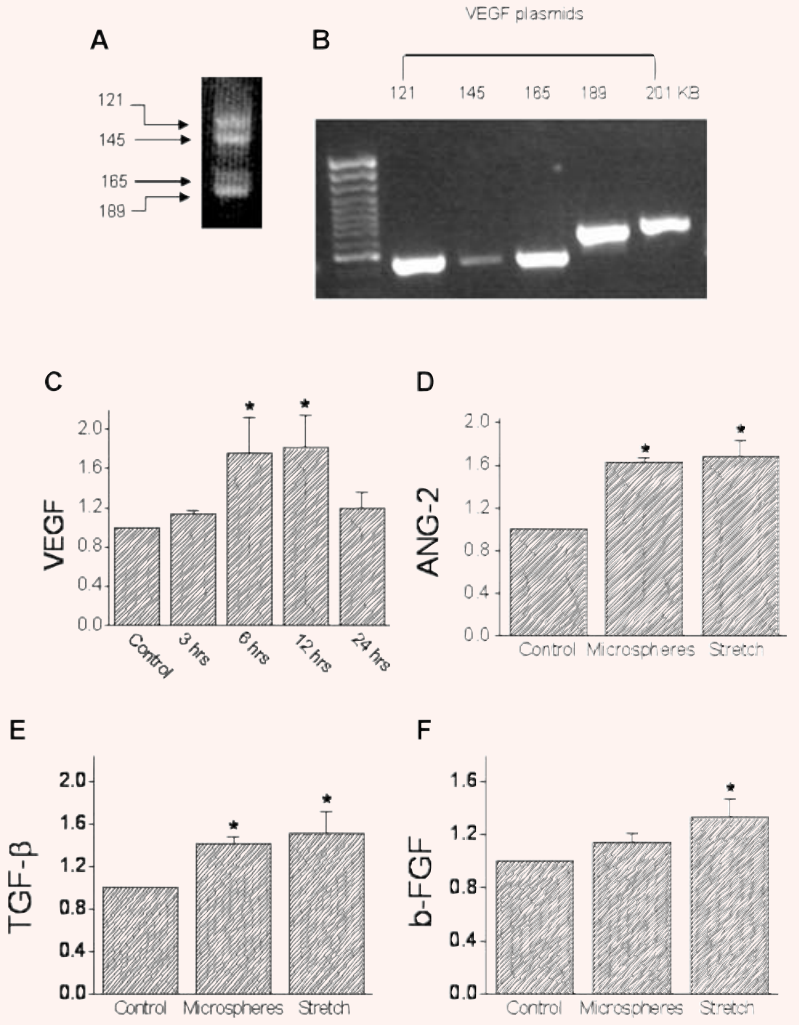

Fig. 6 The effects of mechanical load on the transcription levels of VEGF, Ang-2, TGF-ß and basic FGF. (**A**) The four bands representing the 121, 145, 165 and 201 KB VEGF forms that were induced by exposing NRVM to microspheres. (**B**) Electrophoresis analysis of five plasmids encoding the five VEGF isoforms (121, 145, 165, 189 and 201 KB). [**C**] The time course of VEGF induction: cultures were exposed to microspheres for 3, 6, 12 and 24 hrs, mRNA was extracted, and RT-PCR performed (see Table 1 for details). The amplified products were normalized to actin mRNA. The results are expressed as fold of the control. (**D**) Ang-2; (**E**) TGF- β; (F) b-FGF. In (**D**)–(**F**), experimental details as in (**C**). * $P<0.05$, compared to control. n = 10 experiments.

Conditioned medium from NRVM exposed to microspheres causes angiogenesis

To address the question whether the angiogenic factors secreted by the mechanical load are functional, we tested whether conditioned medium collected from microspheres-treated NRVM causes angiogenesis. In these experiments, BAEC were incubated with conditioned medium collected from cultures exposed for 24 hrs to microspheres, pulsatile cyclic stretch or from control untreated cultures. The effect of the conditioned medium on endothelial cell migration (a key step towards growing new blood vessels) was tested using the cellular injury assay. As seen in Figure 7A, conditioned media from microspheres-treated cultures increased endothelial cell migration by 15% ($P<0.05$). Next, we determined the effect of conditioned medium from microsphere-treated (compared to control) cultures on tube formation in endothelial cell cultures, which is a common assay for testing the angiogenic potential of endothelial cells [23]. As shown by two representative experiments (Fig. 7B) and by the summary of five

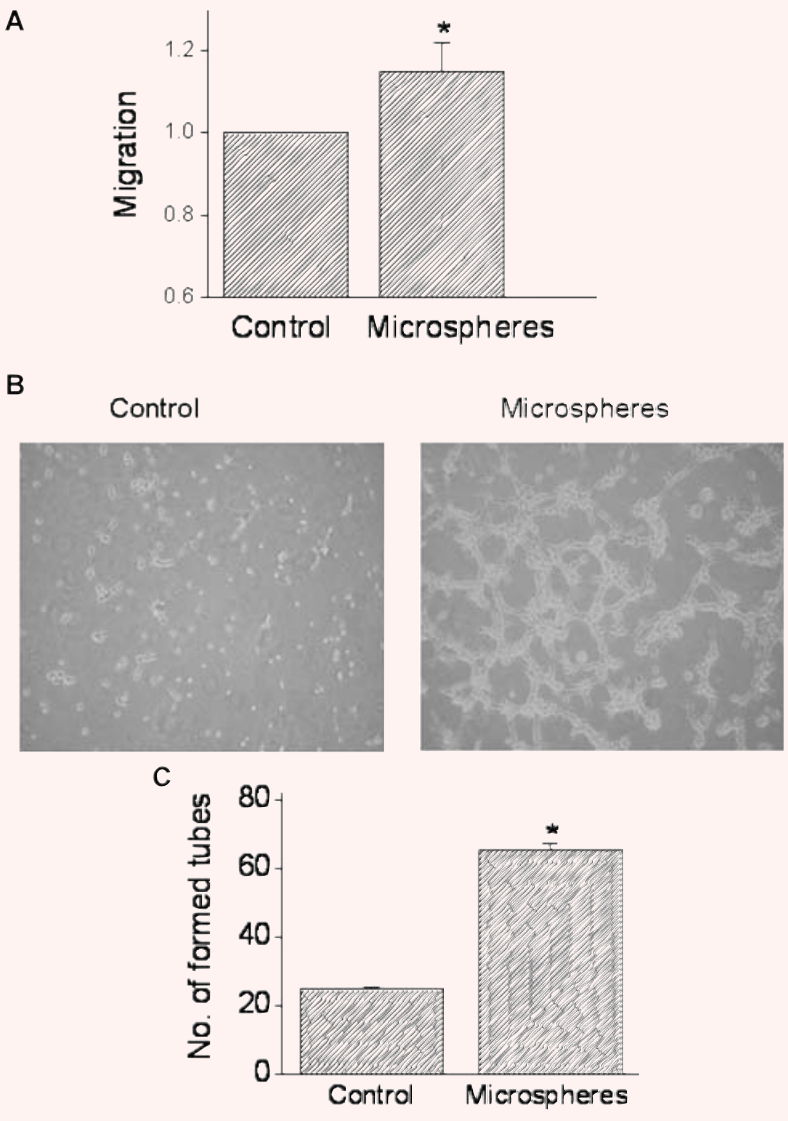

Fig. 7 The effect of conditioned media from NRVM exposed to microspheres on endothelial cells migration and tube formation. (**A**) The effect of mechanical load on endothelial cells migration (see Methods for details). The cultures were incubated with the conditioned media for 24 hrs and cell migration was determined as the distance between the non-scraped cells to the edge of each well. The rate of migration caused by microspheres-derived conditioned medium is expressed as fold of the conditioned medium from control cultures. (**B**) and (**C**) The effect of conditioned media on tube formation. (**B**) Photomicrographs of the new tubes following the incubation of the BAECs cultures for 5 hrs with control conditioned medium or with conditioned media from microspheres-treated cultures. (**C**) The effect of the conditioned media (following 5 hrs incubation) on the number of newly formed tubes was expressed as the number of tubes counted in three fields, in three different wells. * $P<0.05$, compared to control. n = 5 experiments.

experiments (Fig. 7C), conditioned medium from microspheres-treated cultures caused a more prominent ($P<0.05$) tube formation than the control medium.

Discussion

In the present study we tested the hypothesis that mechanical load simulating pressure-overload, which is different from static or cyclic stretch (simulating preload), can cause the production of angiogenic factors by ventricular myocytes. Specifically, we investigated whether mechanical load generated by glass microspheres on ventricular myocytes can lead to a paracrine interaction between myocytes and endothelial cells which is capable of generating new blood vessels.

The experimental model-induction of mechanical load by glass microspheres

While a detailed analysis of the physical interactions between glass microspheres and the myocyte is beyond the scope of this article, it is evident that the type of force induce by the microspheres is

complex. In principle, the cell is subjected to both shear, as well as compression and tension loads. If we assume that the microsphere and the cell are connected at one rigid point, than a local shear force is the dominant load. However, in the current experimental settings, the interface between the microsphere and the cell is distributed along a larger region and in some cases in which the microsphere is engulfed by the cell membrane, the compression and tension forces are the dominating forces. In cases where the dominant force is shear, it is different from shear force that is caused by flow over the cell outer surface, in that the force is both local and restricted to the time of cell contraction. Further, the load imposed on the myocytes acts only during myocyte contraction regardless of the beating frequency, and therefore by definition, such a load can be regarded as an afterload. In previous studies, the major means for exerting mechanical load on cultured myocytes were static [8–11] and cyclic stretch [12–14]. In these models in contrast to ours, due to the lack of synchronization with the myocytes' contracting cycle, the imposed load was of a combined nature: preload and afterload. Since exerting overload by means of glass microspheres is not limited to any particular apparatus or bath, and is independent of an external power source, it allows versatile experimental protocols (in addition to the protocols presented here) such as: (1) sequential, non-invasive monitoring of the effect of the mechanical load on contractile (using video edge detector) and electrophysiological properties by means of the MEA technology [20, 21]; (2) investigating the effect of mechanical load on gap junctional or cytoskeletal elements trafficking/migration, by means of time-lapse life confocal microscopy of GFP-tagged molecules.

The force generated by glass microspheres

Recently Wang and co-workers [15]—the first group to utilize glass microspheres to impose a quantifiable load on isolated myocytes, calculated the resistive load induced by the microspheres to be in the order of 10^{-10}N/μm^2. With an estimated NRVM dimension of 40 μm $\times$ 40 μm, a single microsphere causes a resistive force of 1.6×10^{-10} Newton. The maximal force acting on the myocyte by a single microsphere in our model system was calculated to be 2.4×10^{-8} Newton and Frms was 0.85×10^{-8} Newton (at a stimulation rate of 1 Hz). As in our study the microspheres were spread at an estimated density of ~3000 microspheres/mm^2, the maximal force imposed per area by the microspheres is 7.2×10^{-8}N/μm^2. The difference between the two calculated forces (ours is much larger than Wang's *et al.*) may result from the fact that in the present study: (1) the microsphere density was much higher (in order to cover a larger area of the culture); (2) the collagen-coated microspheres strongly adhered to, and hence moved as part of the contracting cells. In contrast, in Wang's study the microspheres were sliding on the myocytes, and therefore the friction forces played a larger part than the inertial forces which were the major forces in our model system.

The mechanical load generated by glass microspheres does not cause hypertrophy

Numerous studies have shown that cyclic stretch of cardiac myocytes causes hypertrophy which was shown to be mediated by tyrosine kinases, mitogen-activated protein kinase (MAPKs), protein kinase C and phospholipases C and D [7, 13, 39–41]. Using an identical experimental system in NRVM, Zhuang *et al.* showed that in addition to the hypertrophic response, cyclic stretch caused a dramatic up-regulation of Cx43 after only 1 hr, and a further increase after 6 hrs [14]. In agreement with the lack of hypertrophy in our study, microspheres did not increase total Cx43 and non-phosphorylated Cx43 protein expression or the Cx43 fluorescence signal area and intensity.

The effects of glass microspheres on the $[Ca^{2+}]_i$ transients

The main effects of microspheres on the $[Ca^{2+}]_i$ transients were to increase diastolic and systolic fluorescence ratios as well as to decrease the rate of the relaxation. After 24 hrs, microspheres also caused arrhythmias which were abolished at high stimulation rates, suggesting that they were triggered by early afterdepolarizations. We thus speculate that at least some of the abovementioned changes can be accounted for by reduced SR Ca-ATPase activity, shown to occur in ventricular myocytes from rats which underwent aortic banding [42]. For example, the increased diastolic $[Ca^{2+}]_i$ and the attenuated rate of the $[Ca^{2+}]_i$ transients relaxation can be caused by a decreased rate of Ca^{2+} uptake into the SR. In agreement with this notion is the generation of early afterdepolarizations known to be triggered by increased diastolic $[Ca^{2+}]_i$ which promotes membrane potential oscillations [43, 44].

Glass microspheres do not affect action potential propagation in NRVM

As the final step in characterizing the experimental model, we investigated the effect of microspheres on action potential propagation by means of the MEA data acquisition system. As shown in Figures 5C and D, in agreement with the results described so far showing that microspheres do not cause hypertrophy, conduction velocity was not altered throughout the 24 hrs exposure period to microspheres. In contrast, using identical stretch apparatus Kléber's group [14] showed that conduction velocity increased from 27 cm/sec in control cultures to 35 cm/sec after 1 hr of stretch and to 37 cm/sec after 6 hrs.

Glass microspheres release angiogenic factors and cause angiogenesis: comparison to cyclic stretch

Several studies demonstrated that mechanical loading of cultured cardiac myocytes causes secretion of VEGF as well as other angiogenic-promoting growth factors [6, 45, 46]. For example, Zheng *et al*. stretched NRVM by means of the *Flexercell Stretch Unit*, and found that after 1 hr of stretch, VEGF (but not b-FGF) and TGF-β increased 2–2.5 fold [6]. As previously proposed, TGF-β mediates VEGF secretion by cardiac myocytes [47]. In agreement with Zheng *et al*., van Wamel *et al*. showed in the same experimental system that 4 hrs of cyclic stretch increased the expression of TGF-β by 21% [48]. Finally, Kléber's group showed that after 6 hrs of stretch, VEGF content of the culture medium increased by 4-fold [45]. In agreement with previous findings, we demonstrate here (Fig. 6) that mechanical load, other than cyclic stretch, induced by microspheres, increased VEGF mRNA levels. This 2-fold increase in VEGF mRNA is compatible with increase in VEGF protein expression reported previously. In addition to VEGF, microspheres also increased the mRNA levels of TGF-β and Ang-2 (the Tie2 ligand), but not of b-FGF. As seen in Figure 6, cyclic stretch increased the mRNA levels of Ang-2 (in agreement with Zheng *et al.* [7]), TGF-β and b-FGF.

Microsphere-induced secreted factors cause angiogenesis

In support of the previous findings, we showed that both cyclic stretch and microspheres increased the expression of several factors which have important roles in angiogenesis. In brief, VEGF is a potent endothelial cell specific mitogen and a critical factor in collateral formation [reviewed in 32, 49, 50]. Ang-2 is expressed along with VEGF at vascular remodelling sites [6] and probably blocks the stabilizing action of Ang-1, and thereby contributes to vascular remodelling. TGF-β is a factor known to be critical for vascular development is a potent inducer of VEGF and can affect VEGF expression in an autocrine manner [32]. Finally, b-FGF which is highly expressed during prenatal and early postnatal periods was not increased by microspheres.

A strong support for the notion that microspheres generate mechanical force capable of releasing angiogenic factors is the marked increase (~ 3-fold) in tube formation caused by conditioned media collected from microsphere-treated cultures (Fig. 7). The increased tube formation reported here resembles Zheng's *et al*. findings. These authors found that after 6–8 days of treatment with conditioned media from stretched NRVM, coronary microvascular endothelial cells 'appeared in networks of cords' [6]. While the authors verified that these cell cords formed tubular structures by transmission electron microscopy, no quantitative analysis was provided. A key disparity between the two studies is that here tube formation was evident as early as 1 hr (data not shown) after addition of the conditioned media and prominent at 6 hrs, whereas Zheng *et al*. reported increased tube formation after 6–8 days; this major difference may result from the fact that as far as angiogenesis is concerned, conditioned medium from microspheres-treated NRVM is more potent than that from cyclic stretched myocytes.

In summary, we showed that: (1) mechanical load induced by glass microspheres in NRVM increased the expression of several angiogenic factors; (2) conditioned medium from microspheres-treated NRVM caused angiogenesis. These findings support a mechanical load-activated paracrine interaction between cardiac myocytes and endothelial cells, which *in vivo* can contribute to augmented angiogenesis under conditions of mechanical overload. Finally, based on the results of the present work, this experimental model can be further employed to investigate the interaction between mechanical overload, increased expression of growth factors and angiogenesis.

Acknowledgements

This work was supported by the Rappaport Family Institute for Research in the Medical Sciences, the German-Israel Foundation (to O.B, S.K and J.S) and the US-Israel Binational Science Foundation (to O.B).

References

1. **Carmeliet P.** Mechanism of angiogenesis and arteriogenesis. *Nat Med.* 2000; 6: 389–95.
2. **Aird WC, Edelberg JM, Weiler-Guettler H, Simmons WW, Smith TW, Rosenberg RD.** Vascular bed-specific expression of an endothelial cell gene is programmed by the tissue microenvironment. *J Cell Biol.* 1997; 38: 1117–24.
3. **Brogi E, Schatteman G, Wu T, Kim EA, Varticovski L, Keyt B, Inser JM.** Hypoxia-induced paracrine regulation of vascular endothelial growth factor receptor expression. *J Clin Invest.* 1996; 97: 469–76.
4. **Edelberg JM, Aird WC, Wu W, Rayburn H, Mamuya WS, Mercola M, Rosenberg RD.** PDGF mediates cardiac microvascular communication. *J Clin Invest.* 1998; 102: 837–43.
5. **Guillot PV, Guan J, Liu L, Kuivenhoven JA, Rosenberg RD, Sessa WC, Aird WC.** A vascular bed-specific pathway. *J Clin Invest.* 1999; 103: 799–5.
6. **Zheng W, Seftor EA, Meininger CJ, Hendrix MJ, Tomanek RJ.** Mechanisms of coronary angiogenesis in response to stretch: role of VEGF and TGF-beta. *Am J Physiol Heart Circ Physiol.* 2001; 280: 909–17.
6. **Zheng W, Christensen LP, Tomanek RJ.** Stretch induces up regulation of key tyrosine kinase receptors in microvascular endothelial cells. *Am J Physiol Heart Circ Physiol.* 2004; 287: 2739–45.

7. **Komuro I, Kaida T, Shibazaki Y, Kurabayashi M, Katoh Y, Hoh E, Takaku F, Yazaki Y.** Stretching cardiac myocytes stimulates protooncogene expression. *J Biol Chem.* 1990; 265: 3595–8.
8. **Malhotra R, Sadoshima J, Brosius F. C III, Izumo S.** Mechanical stretch and angiotensin II differentially upregulate the renin-angiotensin system in cardiac myocytes *in vitro*. *Circ Res.* 1999; 85: 137–46.
9. **Miyata S, Haneda T, Osaki J, Kikuchi K.** Renin-angiotensin system in stretch-induced hypertrophy of cultured neonatal rat heart cells. *Eur J Pharmacol.* 1996; 307: 81–8.
10. **Tsuruda T, Kato J, Kitamura K, Imamura T, Koiwaya Y, Kangawa K, Komuro I, Yazaki Y, Eto T.** Enhanced adrenomedullin production by mechanical stretching in cultured rat cardiomyocytes. *Hypertension.* 2000; 35: 1210–4.
11. **Liang F, Wu J. Garami M, Gardner DG.** Mechanical strain increases expression of the brain natriuretic peptide gene in rat cardiac myocytes. *J Biol Chem.* 1972; 272: 28050–6.
13. **Shyu KG, Chen JJ, Shih N. L, Wang DL, Chang H, Lien WP, Liew CC.** Regulation of human cardiac myosin heavy chain genes by cyclical mechanical stretch in cultured cardiocytes. *Biochem Biophys Res Commun.* 1995; 210: 567–73.
14. **Zhuang J, Yamada KA, Saffitz JE, Kléber AG.** Pulsatile stretch remodels cell- to-cell communication in cultured myocytes. *Circ Res.* 2000; 87: 316–22.
15. **Wang Z, Lam CF, Mukherjee R, Hebbar L, Wang Y, Spinale FG.** Relationship between external load and isolated myocyte contractile function with CHF in pigs. *Am J Physiol Heart Circ Physiol.* 1997; 273: 183–191.
16. **Yaniv G, Shilkrut M, Lotan R, Berke G, Larisch S, Binah O.** Hypoxia predisposes neonatal rat ventricular myocytes to apoptosis induced by activation of the Fas (CD95/Apo-1) receptor: Fas activation and apoptosis in hypoxic myocytes. *Cardiovasc Res.* 2002; 54: 611–23.
17. **Dewey CF, Jr., Bussolari SR, Gimbrone MA, Jr., Davies PF.** The dynamic response of vascular endothelial cells to fluid shear stress. *J Biomech Eng.* 1981; 103: 177–85.
18. **Shanker AJ, Yamada K, Green KG, Yamada KA, Saffitz JE.** Matrix-protein-specific regulation of Cx43 expression in cardiac myocytes subjected to mechanical load. *Circ Res.* 2005; 96: 558–66.
19. **Felzen B, Shilkrut M, Less H, Sarapov I, Maor G, Coleman R, Robinson RB, Berke G, Binah O.** Fas (CD95/Apo-1)–mediated damage to ventricular myocytes induced by Cytotoxic T Lymphocytes from perforin-deficient Mice: A major role for inositol 1,4,5-trisphosphate. *Circ Res.* 1998; 82: 438–50.
20. **Meiry G, Reisner Y, Feld Y, Goldberg S, Rosen M, Ziv N, Binah O.** Evolution of action potential propagation and repolarization in cultured neonatal rat ventricular myocytes. *J Cardiovasc Electrophysiol.* 2001; 12: 1269–77.
21. **Zeevi-Levin N, Barac DY, Reisner Y, Reiter I, Yaniv G, Meiry G, Abassi Z, Kostin S, Schaper J, Rosen MR, Resnick N, Binah O.** Gap junctional remodeling by hypoxia in cultured neonatal rat ventricular myocytes. *Cardiovasc Res.* 2005; 66: 64–73.
22. **Comber BL, Gotlieb AI.** *In vitro* endothelial wound repair. Interaction of cell migration and proliferation. *Arteriosclerosis.* 1990; 10: 215–22.
23. **Ashton AW, Yokota R, John G, Zhao S, Suadicani SO, Spray DC, Ware JA.** Inhibition of endothelial cell migration, intercellular communication, and vascular tube formation by thromboxane A(2). *J Biol Chem.* 1999; 274: 35562–70.
24. **Barac DY, Zeevi-Levin N, Yaniv G, Reiter I, Milman F, Shilkrut M, Coleman R, Abassi Z, Binah O.** The 1,4,5-inositol trisphosphate pathway is a key component in Fas-mediated hypertrophy in neonatal rat ventricular myocytes. *Cardiovasc Res.* 2005; 68: 75–86.
25. **Fink C, Ergun S, Kralsch D, Remmers U, Weil J, Eschenhagen T.** Chronic stretch of engineered heart tissue induces hypertrophy and functional improvement. *FASEB J.* 2000; 214: 669–79.
26. **Sadoshima J XY, Slayter HS, Izumo S.** Autocrine release of angiotensin II mediates stretch-induced hypertrophy of cardiac myocytes *in vitro*. *Cell.* 1993; 75: 977–84.
27. **Asakawa M, Takano H, Nagai T, Uozumi H, Hasegawa H, Kubota N.** Peroxisome proliferator-activated receptor gamma plays a critical role in inhibition of cardiac hypertrophy *in vitro* and *in vivo*. *Circulation.* 2002; 105: 1240–6.
28. **Okoshi MP, Yan X, Okoshi K, Nakayama M, Schuldt AJT, O'Connell TD, Simpson PC, Lorell BH.** Aldosterone directly stimulates cardiac myocyte hypertrophy. *J Cardiac Failure.* 2004; 10: 511–8.
29. **Tongers J, Fiedler B, König D, Kempf T, Klein G, Heineke J, Kraft T, Gambaryan S, Lohmann SM, Drexler H, Wollert KC.** Heme oxygenase-1 inhibition of MAP kinases, calcineurin/NFAT signaling, and hypertrophy in cardiac myocytes. *Cardiovasc Res.* 2004; 63: 545–52.
30. **Xie K, Wei D, Shi Q, Huang S.** Constitutive and inducible expression and regulation of vascular endothelial growth factor. *Cytokine Growth Factor Rev.* 2004; 15: 297–324.
31. **Luodonpaa M, Vuolteenaho O, Eskelinen S, Ruskoaho H.** Effects of adrenomedullin on hypertrophic responses induced by angiotensin II, endothelin-1 and phenylephrine. *Peptides.* 2001; 122: 1859–66.
32. **Seko Y, Takahashi N, Tobe K, Kadowaki T, Yazaki Y.** Pulsatile stretch activates mitogen-activated protein kinase (MAPK) family members and focal adhesion kinase (p125(FAK)) in cultured rat cardiac myocytes. *Biochem Biophys Res Commun.* 1999; 259: 8–14.
33. **Van Wamel AJ RC, Van der Valk-Kokshoom LE, Schrier PI, Van der Laarse A.** The role of angiotensin II, endothelin-1 and transforming growth factor-β as autocrine/paracrine mediators of stretch-induced cardiomyocyte hypertrophy. *Mol Cell Biochem.* 2001; 218:113–24.
34. **Saffitz JE, Kléber AG.** Effects of mechanical forces and mediators of hypertrophy on remodeling of gap junctions in the heart. *Circ Res.* 2004; 94: 585–91.
35. **Keung EC.** Calcium current is increased in isolated adult myocytes from hypertrophied rat myocardium. *Circ Res.* 1989; 64: 753–63.
36. **Schwarz B, Percy E, Gao XM, Dart AM, Richardt G and Du XJ.** Altered calcium transient overload. *Europ J Heart Fail.* 2003; 5: 131–6.
37. **Tomaselli GF, Marbán E.** Electrophysiological remodeling in hypertrophy and heart failure. *Cardiovasc Res.* 1999; 42: 270–83.
38. **Carmeliet P, Collen D.** Molecular Basis of Angiogenesis: Role of VEGF and VE-Cadherin. *Ann NY Acad Sci.* 2000; 902: 249–64.
39. **Komuro I, Kudo S, Yamazaki T, Zou Y, Shiojima I, Yazaki Y.** Mechanical stretch activates the stress-activated protein kinases in cardiac myocytes. *FASEB J.* 1996; 10: 631–6.
40. **Ruwhof C, van der Laarse A.** Mechanical stress-induced cardiac hypertrophy: mechanisms and signal transduction pathways. *Cardiovasc Res.* 2000; 47: 23–37.
41. **Sadoshima J, Jahn L, Takahashi T, Kulik TJ, Izumo S.** Molecular characterization of the stretch-induced adaptation of cultured cardiac cells. An *in vitro* model of

load-induced cardiac hypertrophy. *J Biol Chem.* 1992; 267: 10551–60.

42. **McCall E, Ginsburg KS, Bassani RA, Shannon TR, Qi M, Samarel AM, Bers DM.** Ca flux, contractility, and excitation-contraction coupling in hypertrophic rat ventricular myocytes. *Am J Physiol Heart Circ Physiol.* 1998; 274: H1348–60.
43. **January CT, Riddle JM.** Early afterdepolarization: mechanism of induction and block. *Circ Res.* 1989; 64: 977–990.
44. **Wu J, Wu J, Zipes DP.** Early afterdepolarization, U wave, and torsades de pointes. *Circulation.* 2002; 105: 675–6.
45. **Pimentel RC, Yamada KA, Kléber AG, Saffitz JE.** Autocrine regulation of myocyte Cx43 expression by VEGF. *Circ Res.* 2002; 90: 671–7.
46. **Seko Y, Seko Y, Fujikura H, Pang J, Tokoro T, Shimokawa H.** Induction of vascular endothelial growth factor after application of mechanical stress to retinal pigment epithelium of the rat *in vitro*. *Invest Ophthalmol Vis Sci.* 1999; 40: 3287–91.
47. **Li J, Hampton T, Morgan JP, Simons M.** Stretch-induced VEGF Expression in the heart. *J Clin Invest.* 1997; 100: 18–24.
48. **van Wamel AJ, Ruwhof C, van der Valk-Kokshoorn LJ, Schrier PI, van der Laarse A.** Stretch-induced paracrine hypertrophic stimuli increase TGF-beta1 expression in cardiomyocytes. *Mol Cell Biochem.* 2002; 236: 147–53.
49. **Costa C, Soares R, Schmitt F.** Angiogenesis: now and then. *Apmis.* 2004; 112: 402–12.
50. **Ziche M, Donnini S, Morbidelli L.** Development of new drugs in angiogenesis. *Curr Drug Targets.* 2004; 5: 485–93.